

Assessment of the real contact area of a multi-contact interface from electrical measurements

BRICE JONCKHEERE¹, ROBERT BOUZERAR¹, VALERY BOURNY^{2,3},
THOMAS BAUSSERON⁴, NICOLAS FOY^{5,3}, OLIVER DURAND-DROUHIN¹,
FRANCOISE LE MARREC¹, EDDY CHEVALLIER⁶

¹ : Laboratoire de Physique de la Matière Condensée, Université de Picardie Jules Verne (UPJV),
Amiens, France

² : Laboratoire des Technologies Innovantes (LTI, EA3899), UPJV, Saint-Quentin, France

³ : ESIEE-Amiens, Amiens, France

⁴ : SNCF Direction de l'Ingénierie - Traction Electrique IPTE, Saint-Denis, France

⁵ : Laboratoire de Physique des Systèmes Complexes, UPJV, Amiens, France

⁶ : Département de physique, UPJV, Amiens, France

Abstract - The electrical supply of moving trains is provided by a sliding contact between the train's pantographs and the catenary. This electromechanical interface is composed of the strips of the pantograph – made mainly of carbon – and the catenary contact wire. The objective is to define the real contact area with a simple electrical measurement. In many practical or fundamental situations involving contacting solids, the relevant notion of the real contact area is a very delicate one and especially its experimental assessment.

Based on Drude's classical transport model and within the linear elasticity approximation, a phenomenological model of a metal/metal contact is built up, offering an interpretation framework of experimental data. The model accounts for the influence of the mechanical state of the contacting zone upon its electrical properties, such as its impedance. Interpreting available data within this framework leads to the assessment of the number of spots. The total contact force works on the spots and on the average contact length. In this model, the interface is treated as a new medium with its own conductivity.

Key words: multi-contact / real contact area / interface / spots / electrical measurement

Nomenclature

A : real contact area [m^2]

C : Capacitance of the interface [F]

C_H : Holm's capacitance [F]

C_Q : Quantum capacitance [F]

$\bar{G}(E_F)$: The Fermi level density of states per unit volume [$\text{J}^{-1}.\text{m}^{-1}$]

h : Spot height [μm]

i : Imaginary number [dimensionless]

L_D : Drude's Inductance [μH]

L_{eff} : Inductance effective [μH]

N : Number of spots [dimensionless]

R : Resistance of one spot [Ω]

R_{eq} : Resistance of electrical analog [Ω]

R_{int} : Resistance of the interface [Ω]

S : Contact surface of one spot [m^2]

Sa : The Average Roughness [μm]

Z_{int} : Interface impedance [Ω]

γ : Conductivity [$\Omega^{-1}.\text{m}^{-1}$]

γ_D : Drude's Conductivity [$\Omega^{-1}.\text{m}^{-1}$]

ρ : Resistivity [$\Omega.\text{m}$]

τ : Drude's relaxation time [s]

ω : Angular frequency [$\text{rad}.\text{s}^{-1}$]

1. Introduction

Pantograph catenary systems have been used for a long time in railway systems. The pantograph systems are used to transfer the electrical energy from the catenary system to the train. A contact force must occur between the pantograph and the contact wire of the catenary for a train to move on an electrical railway system. Consequently, appropriate measures to reduce wear should be taken into account. This will extend the lifetime of the equipment and reduce the maintenance and repair costs. [1-4] To achieve better control of the pantograph-catenary interaction, the contact force should be known.

Unluckily, a direct assessment of the force acting on the contact zone is made difficult by its restricted accessibility. To address properly this complex issue, the measurement of any appropriate physical quantity sensitive to the mechanical state of the interface is required. Electrical and/or thermal resistance of a metal/metal contact interface can fulfill these requirements since it mirrors the mechanical conditions imposed to the interface. For instance, the dependence of the interface resistance upon the applied compression forces is a well-known effect [5-8]. Fundamentally, a better understanding of the transport properties of such interfaces can lead to a control of the mechanical state through electrical monitoring. Beyond the unwanted effects of unavoidable, wear processes, the physical consequences of the discrete structure of the interface between contacting solids falls within a multi-physical approach. To tackle the different degrees of complexity of these discrete interfaces, a model of the electrical resistance and its correlation with the surface state would be very helpful.

In many industrial applications, the discrete interfaces between contacting solids are often given a tribological and/or a mechanical function and in some cases an electrical function (e.g. for the needs of electrical monitoring). To achieve this goal, the optimization of both mechanical and electrical properties of such interfaces is thus needed, in spite of a limited knowledge.

Because of the complexity of the physical situation, previous research investigated only D.C. [5-8] electrical properties of the contact, and which reveal only limited information about the evolutionary process. Extended investigations based on the impedance response would be of great help for a better understanding of the pantograph–catenary system.

To highlight some fundamental aspects of the electrical transport through a metal/metal interface, we achieved both experimental and theoretical studies of a copper/copper contact. Having in mind the correlation between surface mechanical states and, electrical transport, simultaneous current-voltage characteristics along with a structural analysis of the metallic plates surfaces have been carried out. The experimental results reported in this paper may help understanding the physical mechanisms ruling the electrical contact in pantograph–catenary systems and provide some assessment of relevant quantities such as the number of contacts or the real contact area involved in contacting solids and their dependence upon the applied forces.

2. Materials and methods

2.1. Experimental bench

The objective is to characterize the metal / metal interface and its evolution as a function of the load. To do this, two copper plates of size 25x25x1 mm³ are taken in order to create an interface. For this, an experimental bench was developed as a model system. This model system was developed to put face to face the two copper plates. To extract relevant information about metallic interfaces, AC electrical measurements were performed on a system of two copper plates compressed against each other, using the experimental configuration schematized in Figure 1. For this purpose, a dedicated experimental bench was designed specifically. This device brings two copper sheets closer until the contact is established. At this moment, there is an electrical transition, the phase change between the current and the voltage. These plates are manually compressed by a lever arm from 0 N (when the contact is established) to 15 N. The device allows the measurement of both the electrical contact impedance between the two pieces of copper, using an impedance analyzer Hioki IM 3570. At the interface, many of parameters influences the impedance so, the operating conditions require a low voltage to prevent electrical breakdown [9] due to the small separation between the metal pieces and high temperature. For these reasons, all the measurements were carried out with a voltage of 1 V.

2.2. Profilometer

Due to their surface roughness, the contact interface between two solids under compression is of discrete nature and exhibits a complex structure arising from the random distribution of the spots position, their sizes and shapes [10-11]. The total number of spots (or equivalently the total contact area) as well as their sizes depend on many parameters like the force, the macroscopic shape of the surfaces, the fluctuations of the geometry of the surfaces (roughness), the mechanical properties of materials (hardness, Young's modulus). In this case, a better knowledge of the surface hilly landscape is required. Using a Bruker DEKTAK XT profilometer, the surface geometries of our solids have been inspected. The radius of the stylus is 2 μm and the maps are normalized to $1 \times 1 \text{ mm}^2$ with a resolution of 1 μm in the x and y directions.

3. Results

3.1. Constant force

Setting the applied force to a fixed value at 6 N, the electrical impedance is recorded for excitation frequencies lying within the range 4 Hz - 20 kHz. The frequency range must be low compared to the relaxation time of the Drude model to prevent new effects at the interface. Figure 2 a) shows the real and imaginary parts of the impedance of the plates as functions of the frequency. The drift of the real part can be explained by the error introduced by the measuring instrument. In this case, the simplest electrical equivalent is an RL circuit schematized in Figure

2 b). So, the average of the real part is equivalent to the resistance which gives 1.3 mΩ. An equivalent inductance $L = \frac{\text{Im}(Z)}{\omega}$ is also deduced, (with $\omega = 2\pi f$) which yields an inductance of 0.15 μH.

3.2. Constant frequency

In this system, there is only the resistance of the interface which is sensitive to the variation of the force that is why, panels composing the Figure 3 account for the influence of the compression force on the electrical contact impedance. The varying force, which is imposed as a ramp force, that is, a force increased at a constant rate with a step of 37 mN. It can be clearly seen that both the resistance and the inductance decrease with the applied force, though in a rather different manner. The decrease in resistance on the Figure 3 a) is much faster than that of the inductance (fig.3 b). Indeed, the resistance is clearly reduced by two orders of magnitude. It is worth to notice, that the imaginary part of the impedance decreases more slightly. As opposed to the fast resistance reduction, which is a known effect [12], the decrease of the inductance is more difficult to understand. Another striking difference regards the fluctuations of the inductance. These differences suggest different mechanisms controlling the decrease of the resistance and the inductance. This conclusion should extend to the inductance variations: as a part of the impedance, it is connected to the resistance variations through the Kramers-Kronig relations [13] (reflecting the constraints imposed by the causality principle). As mentioned previously, the resistance is expected to depend naturally on the real area of contact or, more generally, on the geometry of

the contacting surfaces. To evaluate the influence of the surface state on the contact resistance, it is necessary to connect these features with its own roughness.

3.3. Surface properties

The obtained morphology (fig. 4) tells a lot about the importance of that knowledge on the investigation of the physical behavior of a discrete interface. From a scan of the surface, it is possible to extract different quantities to characterize the surface state, such as the spatial parameters (S-parameters). S-parameters characterize the area based on the vertical deviations of the roughness profile from the mean surface. In our case, we will focus on surface roughness through the "Average roughness" (Sa) with typical values such as $Sa = 0,167 \mu\text{m}$. This allows us to estimate an average height of each peak that can be useful for estimating contact length. This parameter and its fluctuations have a sense only in the absence of any mechanical contact. When initiated, the contact alters the geometry (especially at the spot level) and the thermal and electrical transfer features. For our purpose, the fundamental importance of such a surface characterization relies on one fact: the discrete structure (spots) of the contact zone is determined by the surface geometries of the solids.

4. Discussion

4.1. Assumptions of the electrical model of the interface

A physical model of the interface is necessary to interpret the previous results. In the case of two metal pieces in contact, a simplified view of the discrete spot structure is proposed in Figure 5 a). The surfaces of the solids (especially metals) might be covered with a thin inhomogeneous oxide film [9]. Though we cannot discard additional electrical transfer processes such as tunneling [14], the applied current flows mainly through the mechanical spots generated by contacting asperities. In the present study, we focus on the transfer properties of these mechanical spots. Having in mind workable models as simple as possible, we adopt a simplified view based on electrical analogs of the interface as depicted in Figure 5 a). These analogs are made of a parallel assembly of resistances which mimic the spots and a single capacitor accounting for the presence of the oxide layer and/or any contribution arising from the mechanical contact. To simplify the geometry of the problem, we can consider each contact like an equivalent cylinder with its own height h and area S . Actually, the height h is an effective quantity since the spots have no thickness (asperities crush) but, it can be computed through an adequate model of the constriction effect (e.g. Maxwell/Holm's model) [9]- [15]. However, this issue will not be addressed in the present study emphasizing the search for global electrical analogs of the interface. Furthermore, these contacts are considered independent and circular. To deal in a simple way with the electron A.C. transport properties of the interface, Drude's "classical" model will be used. According to the geometrical simplifications of our model, the resistance of a single spot equated to a cylinder is simply $R = \frac{h}{\gamma S}$. Within the

approximations and other simplifications of our model, the A.C. impedance of the interface reads, according to Drude's model,

$$Z_{int}(\omega) = \frac{h}{\gamma(\omega)S} = \frac{h(1 + i\omega\tau)}{\gamma_D S} = \frac{h}{\gamma_D S} + \frac{h}{\gamma_D S} \omega i \quad (1)$$

where the A.C. conductivity $\gamma_\omega = \frac{\gamma_D}{1+i\omega\tau}$ and γ_D is the D.C. Drude conductivity of the metal pieces. In this expression, the resistances only were taken into account. The extension to an arbitrary number of spots N leads to the expression

$$Z_{int}(\omega) = \frac{1}{N \overline{\left(\frac{S}{h}\right)} \gamma_D} + \frac{\tau}{N \overline{\left(\frac{S}{h}\right)} \gamma_D} i\omega \quad (2)$$

In this expression, the quantity $N \overline{\left(\frac{S}{h}\right)} = \sum_{k=1}^N \frac{S_k}{h_k}$ is averaged over the whole set of cylindrical spots. This last quantity is an effective length. For a more realistic view of the interface, it is possible to supplement the electrical analog with a capacitor (fig 5 b), so that the low-frequency limit ($\omega\tau \ll 1$) of the previous expression of the impedance becomes,

$$Z_{int}(\omega) = \frac{1}{N \overline{\left(\frac{S}{h}\right)} \gamma_D} \left(1 - \frac{C - N \overline{\left(\frac{S}{h}\right)} \gamma_D \tau}{N \overline{\left(\frac{S}{h}\right)} \gamma_D} i\omega \right) \quad (3)$$

From this last expression, it is possible to extract a resistance (real part of the impedance) and an effective inductance connected to its imaginary part. These last parameters are simply given by,

$$R_{int} = \frac{1}{N \overline{\left(\frac{S}{h}\right)} \gamma_D} \quad (4)$$

$$L_{eff} = \frac{C - N \overline{\left(\frac{S}{h}\right)} \gamma_D \tau}{N^2 \overline{\left(\frac{S}{h}\right)}^2 \gamma_D^2} \quad (5)$$

Actually, as we are dealing with metal/metal contacts, this effective inductance incorporates a contribution referred to as the Drude (kinetic) inductance $L_D = \frac{\tau}{N \gamma_D (S/h)}$ which does not have an inductive origin, but is rather connected to the kinetic energy of the electrons [16]. This contribution is a direct consequence of the A.C. regime Drude model applied to the cylindrical spots. The effective inductance can be rewritten as,

$$L_{eff} = |R^2 C - L_D| \quad (6)$$

The main weakness of such a simple model regards the physical origin of the capacitance which remains fuzzy. Further studies of these discrete interfaces are clearly needed. Nevertheless, the overall capacitance C should comprise a contribution C_H (or Holm's capacitance) as required by the constriction effect of the spots. In our case, this capacitance varies as $C_H \propto g \epsilon_0 N \overline{(S/h)}$ (for a parallel assembly of N spots) where g is a factor accounting for the geometry of the spots. This first contribution, expected to be very small, must be supplemented with an extra-contribution ΔC , much greater. Anyway, the contribution C_H provides the physical meaning of the fundamental quantity $N \overline{(S/h)}$ associated with the spots: up to a constant factor, it is proportional to Holm's capacitance which, though very small, gives the irreducible part of the capacitance of the interface arising from the spots. The final effective electrical analog is thus a series R/L circuit. It

is worth noticing that the capacitance was “absorbed” in the effective inductance in which it reduces the influence of the kinetic inductance.

4.2. Interpretation and discussion

With the observed data, we extracted the fundamental quantities $\overline{N(S/h)}$ (from eq.4) and the capacitance C (from eq.5) to reveal their evolution with the compression force. The first quantity was straightforwardly extracted from the values of the resistance R , supposed to retain the only contribution of the spots. The overall capacitance was then assessed from the effective inductance variations with the compression force. The results are presented on Figure 6. The very similar variations of these quantities confirm their mutual dependence, as discussed in the previous section. But, the quantitative differences clearly suggest that the overall capacitance does not only consist of Holm’s capacitance. Indeed, the experimental values leads to an estimate $C_H \approx 10^{-16} F$, much smaller (by several orders of magnitude) than the values reported on the right panel of (fig 6 a). An extra contribution is thus clearly present. The same data allows also to assess Drude’s kinetic inductance $L_D \approx \frac{\tau}{100} = 2,4.10^{-16}$ associated with the spots, expected to be negligible (as compared to the typical scale revealed by our data about

10^{-7} H) because of the smallness of the microscopic time τ . Accordingly, the effective inductance of the spots scales as $L_{\text{eff}} \approx R^2 C$ resulting in a capacitance variation range. Such high values of capacitance (for a very thin interface!) cannot be reached through a classical capacitance (geometrical) but rather arise from a

quantum effect. The notion of quantum capacitance attached to metals [17], if applied to our interface, leads to the assessment $C_Q \approx q^2 \bar{G}(E_F) N(\overline{S/h}) \overline{h^2}$ that is, a capacitance proportional to the Fermi level density of states per unit volume, the last combination of factors giving the total volume of the spots. Setting for copper $\bar{G}(E_F) \approx 10^{54} J^{-1} m^{-3}$ and $C_Q \approx 10^{-3} F$ (according to our data) we find $\overline{h^2} \approx 10^{-14} m^2$ or equivalently a thickness $\sqrt{\overline{h^2}} \approx 10^{-7} = 0,1 \mu m$. The corresponding real contact area is about $A = N(\overline{S/h}) \overline{h^2} \approx a$ that is a few $10^{-12} m^2$. This is a reasonable assessment of the interface's thickness which agrees with the typical roughness of the surface (throw parameters Sa). It is thus interesting to notice that a careful analysis of the electrical data leads among other quantities to an assessment of the surface roughness and the real contact area. This interesting agreement between profilometric and electrical data demands further consideration. The assimilation of the extra contribution ΔC to the quantum capacitance is questionable though it appears to be a relevant hypothesis. Only a comprehensive physical description of the discrete interface should allow to answer these legitimate doubts. More especially, the adequate electrical analog should proceed from such a more detailed approach. A last interesting issue regards the higher amplitude fluctuation regime developing at higher forces. The physical origin of that noise should be investigated carefully since it can arise from different sources: mechanical instabilities of contacting asperities (spots number fluctuations), intrinsic spots' electrical noise. Whatever its origin, the study of that noise effect is an interesting prospect.

5. Conclusion

All results prove that the impedance method contains more information than a simple measure of resistance at the interface. The electrical analogs based on a simplified view make a link between the properties of the impedance and the mechanical states of the interface. The real part of the impedance give the quantity $N\overline{(S/h)}$. This quantity is interesting because it is proportional to the real number of contact. Moreover, the imaginary part of the impedance is proportional of the interface capacity with a range from 10^{-4} to 10^{-1} F that it is compatible with quantum capacitance. With this hypothesis, the calculated height for low compression has the same order of magnitude than the measured one throw the Sa parameter. This made it possible to estimate an interface capacity and a contact length. In the future, a study will be carried out at low compressions to separate the number of contacts and the effective length to estimate the number of contacts in order to obtain a fine characterization of this interface. This will allow us to optimize the catenary-pantograph system by the choice of materials, the optimal strength to apply for a minimum of the resistance as well as other applications.

Reference

- [1] J.P. Massat, T. Nguyen Tajan, H. Maitournam, E. Balmès, 2011, Fatigue Analysis of Catenary Contact Wires for High Speed Trains. *In* Pp. 1–11.
- [2] T. Bausseron, P. Baucour, R. Glises, S. Verschelde, D. Chamagne, Heat Modeling of the Catenary's Contact Wire During the Electrical Power Supply of Trains in Station: V08BT10A096, 2014
- [3] C. Pappalardo, M. Mohil, D. Patel, B. Tinsley, A. Shabana, Contact Force Control in Multibody Pantograph/Catenary Systems, *Journal of Multi-Body Dynamics* 230(4): 307–328, 2016.
- [4] Z. Wang, F. Guo, Z. Chen, A. Tang, and Z. Ren, Research on Current-Carrying Wear Characteristics of Friction Pair in Pantograph Catenary System. *In* 2013 IEEE 59th Holm Conference on Electrical Contacts (Holm 2013) Pp. 1–5, 2013.
- [5] Y. Zeroukhi, E. Napieralska-Juszczak, G. Vega, K. Komez, F. Morganti, S. Wiak, Dependence of the Contact Resistance on the Design of Stranded Conductors, *Sensors* 14(8): 13925–13942, 2014.

- [6] B. Arrazat, B. P. Duvivier, V. Mandrillon, K. Inal, 2011, Discrete Analysis of Gold Surface Asperities Deformation under Spherical Nano-Indentation Towards Electrical Contact Resistance Calculation. *In* 2011 IEEE 57th Holm Conference on Electrical Contacts (Holm) Pp. 1–8.
- [7] Y. Zeroukhi, E. Napieralska-Juszczak, G. Vega, et al, 2014, Dependence of the Contact Resistance on the Design of Stranded Conductors, *Sensors* 14(8): 13925–13942.
- [8] A. Tekaya, Influence de la dimensionnalité et de la complexité d'un réseau sous compression mécanique sur les transports électrique et thermique dans les milieux granulaires métalliques. De l'interface individuelle aux propriétés collectives, 2012.
- [9] R. Holm, *Electric Contacts: Theory and Application*. 4th ed. Softcover of orig. ed. 1967. Springer-Verlag Berlin and Heidelberg GmbH & Co. K.
- [10] W. E. Wilson, S. V. Angadi, R. L. Jackson, 2008, Electrical Contact Resistance Considering Multi-Scale Roughness. *In* 2008 Proceedings of the 54th IEEE Holm Conference on Electrical Contacts Pp. 190–197.
- [11] R. Jackson, J. Streater, 2006, A Multi-Scale Model for Contact between Rough Surfaces. *Wear* 261(11–12): 1337–1347.

- [12] S. Dorbolo, N. Vandewalle, 2005, The Branly Effect and Contacting Grains in a Packing. *In Traffic and Granular Flow*, 03 Pp. 521–524, Springer, Berlin,
- [13] E. Barsoukov, J. Macdonald, *Impedance Spectroscopy: Theory, Experiment, and Applications*. John Wiley & Sons, 2005.
- [14] A. Tekaya, R. Bouzerar, V. Bourny, J. Fortin, K.Bourbatache, Transport Électrique Dans Les Milieux Granulaires: Effect D'une Force de Compression Statique. ResearchGate. AFM, Maison de la Mécanique, accessed January 13, 2017.
- [15] R. Fitzpatrick, 2008, *Maxwell's Equations and the Principles of Electromagnetism*. Jones & Bartlett Publishers.
- [16] W. Ashcroft, N. Mermin, 2011, *Solid State Physics*. Cengage Learning.
- [17] S. Luryi, Quantum Capacitance Devices, 1988, *Applied Physics Letters* 52(6): 501–503.

Caption

Figure 1: diagram of the experimental measurement

Figure 2: Impedance Z as a function of the angular frequency (a); Equivalent circuit with effective inductance $L_{\text{eff}} = 0,15 \mu\text{H}$ and resistance equivalent $R_{\text{eq}} = 1,3\text{m}\Omega$ (b)

Figure 3: Electrical contact impedance as a function of the compression for the copper/copper contact (measuring voltage of 1 V).

Figure 4: Real surface landscape $1 \times 1 \text{ mm}^2$ as obtain from profilometry surface inspection

Figure 5: diagram of the multi-contact system (a); Equivalent circuit of the interface (b)

Figure 6: Holm's capacitance $N(\overline{S/h})$ (a); overall interface capacitance C variations against the applied compression (b)

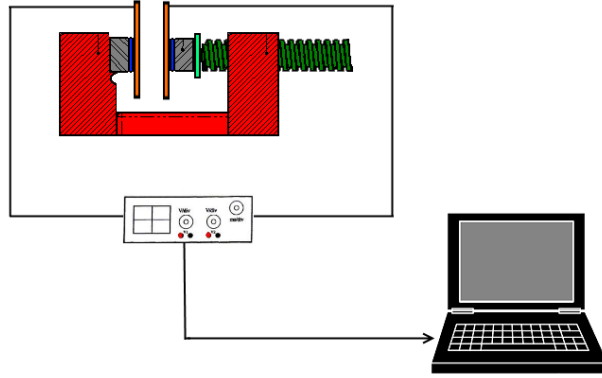
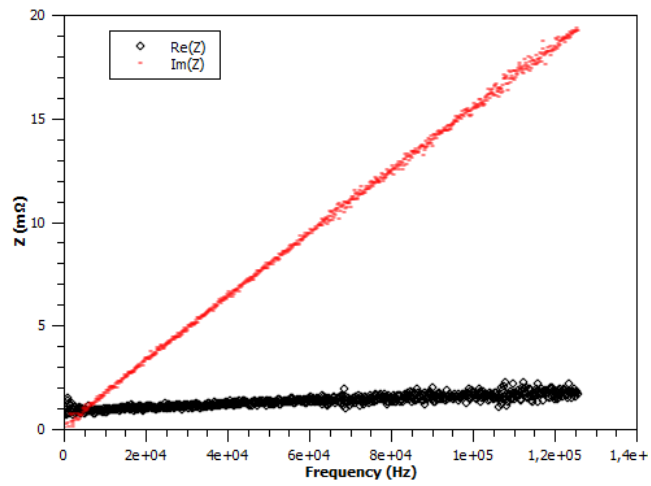
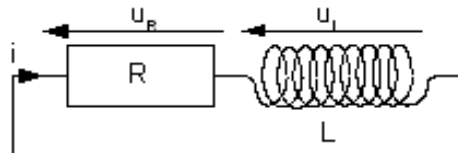


Figure 1

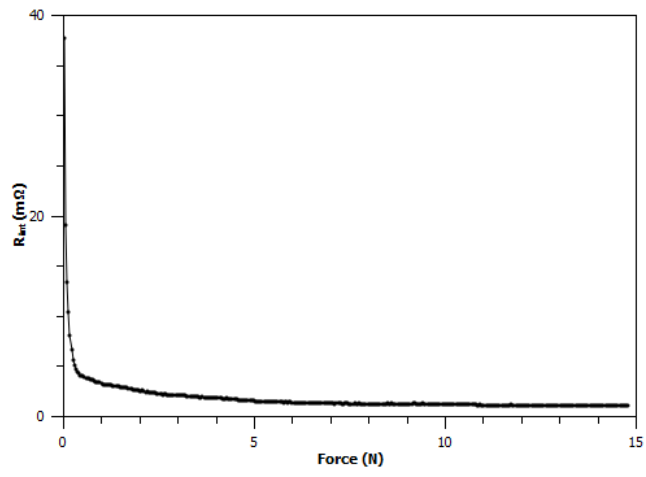


a)

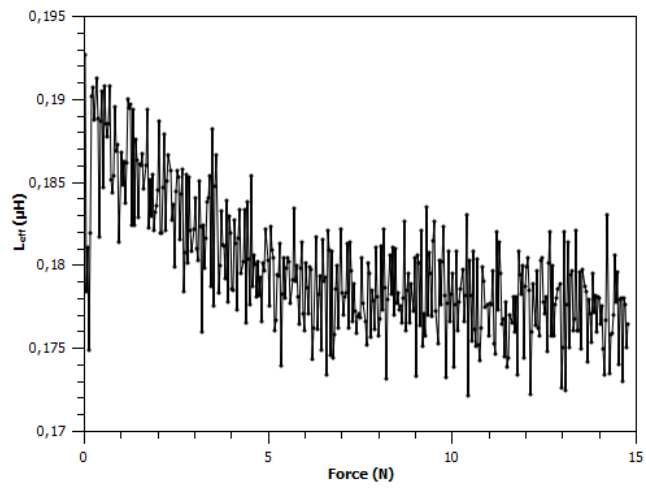


b)

Figure 2



a)



b)

Figure 3

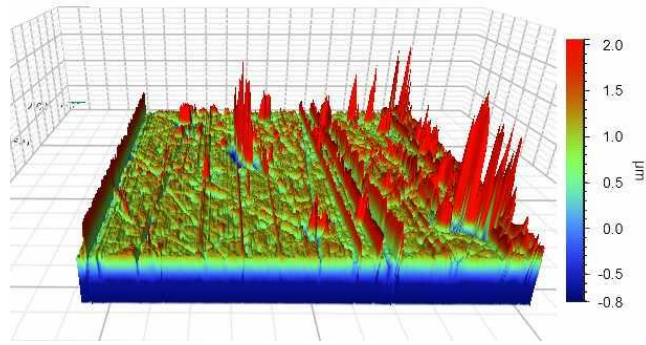
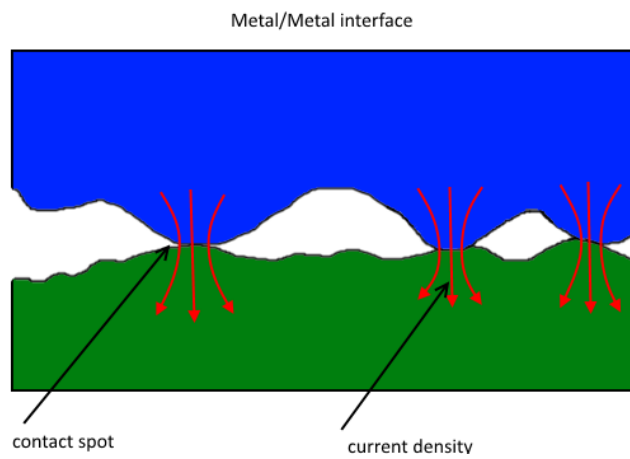
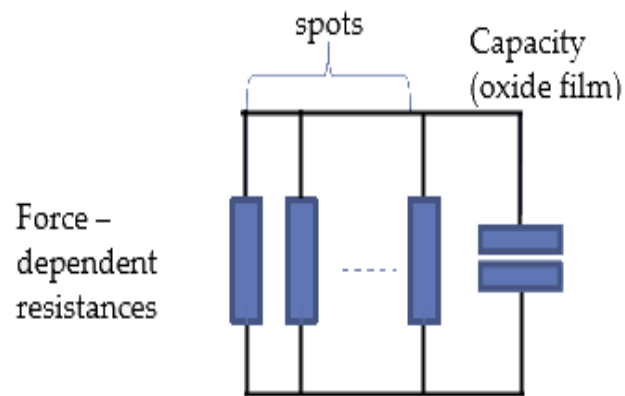


Figure 4

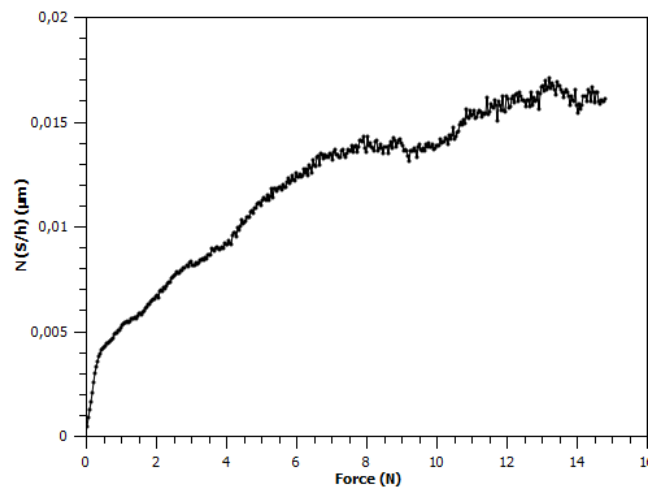


a)

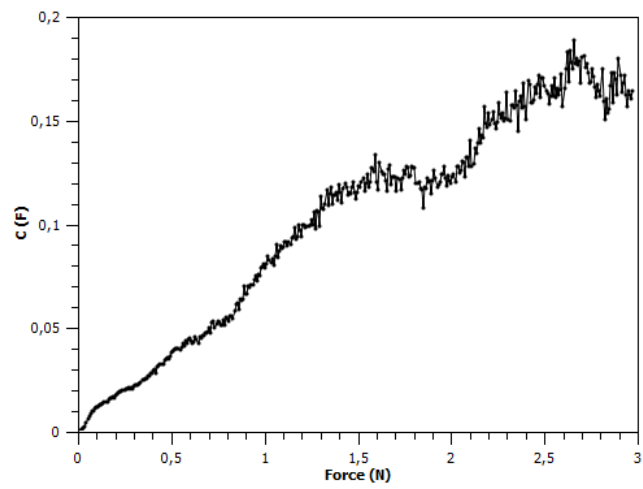


b)

Figure 5



a)



b)

Figure 6